Toxicology and Applied Pharmacology 264 (2012) 232–245

Contents lists available at SciVerse ScienceDirect

Toxicology and Applied Pharmacology

journal homepage: www.elsevier.com/locate/ytaap

Effects of SiC nanoparticles orally administered in a rat model: Biodistribution, toxicity and elemental composition changes in feces and organs

Omar Lozano [a,b,*,1], Julie Laloy [a,c,1], Lütfiye Alpan [a,c], Jorge Mejia [a,b], Stéphanie Rolin [a,c], Olivier Toussaint [a,d], Jean-Michel Dogné [a,c], Stéphane Lucas [a,b], Bernard Masereel [a,c]

[a] Namur Nanosafety Center (NNC), NAmur Research Institute for LIfe Sciences (NARILIS), University of Namur (FUNDP), Rue de Bruxelles 61, B-5000 Namur, Belgium
[b] Research Centre for the Physics of Matter and Radiation (PMR-LARN), University of Namur (FUNDP), Rue de Bruxelles 61, B-5000 Namur, Belgium
[c] Department of Pharmacy, NAMEDIC, Namur Thrombosis and Hemostasis Center (NTHC), University of Namur (FUNDP), Rue de Bruxelles 61, B-5000 Namur, Belgium
[d] Laboratory of Biochemistry and Cellular Biology (URBC), University of Namur (FUNDP), Rue de Bruxelles 61, B-5000 Namur, Belgium

ARTICLE INFO

Article history:
Received 7 May 2012
Revised 30 July 2012
Accepted 6 August 2012
Available online 15 August 2012

Keywords:
SiC nanoparticle
Histopathology
Plasma
Biodistribution
PIXE
Toxicity

ABSTRACT

Background: Silicon carbide (SiC) presents noteworthy properties as a material such as high hardness, thermal stability, and photoluminescent properties as a nanocrystal. However, there are very few studies in regard to the toxicological potential of SiC NPs.
Objectives: To study the toxicity and biodistribution of silicon carbide (SiC) nanoparticles in an *in vivo* rat model after acute (24 h) and subacute (28 days) oral administrations. The acute doses were 0.5, 5, 50, 300 and 600 $mg \cdot kg^{-1}$, while the subacute doses were 0.5 and 50 $mg \cdot kg^{-1}$.
Results: SiC biodistribution and elemental composition of feces and organs (liver, kidneys, and spleen) have been studied by Particle-Induced X-ray Emission (PIXE). SiC and other elements in feces excretion increased by the end of the subacute assessment. SiC did not accumulate in organs but some elemental composition modifications were observed after the acute assessment. Histopathological sections from organs (stomach, intestines, liver, and kidneys) indicate the absence of damage at all applied doses, in both assessments. A decrease in the concentration of urea in blood was found in the 50 $mg \cdot kg^{-1}$ group from the subacute assessment. No alterations in the urine parameters (sodium, potassium, osmolarity) were found.
Conclusion: This is the first study that assesses the toxicity, biodistribution, and composition changes in feces and organs of SiC nanoparticles in an *in vivo* rat model. SiC was excreted mostly in feces and low traces were retrieved in urine, indicating that SiC can cross the intestinal barrier. No sign of toxicity was however found after oral administration.

Introduction

Nanomaterials (NMs) are actively used for a wide variety of applications such as biocompatible materials (Heublein et al., 1998), textile functionalization (Avila and Hinestroza, 2008), coatings against UV radiation or allowing microbial degradation (Nel et al., 2006), and drug delivery (Wang et al., 2009). This unprecedented progress has been associated with concerns about the possible health impacts of NMs. Nanotoxicology has been developed as a specific field of study in light of reports indicating that NMs may generally be more toxic than larger sized particles (Oberdörster, 2001).

Silicon carbide (SiC) presents noteworthy properties as a material such as high hardness, thermal stability, and photoluminescent properties as a nanocrystal (Fan et al., 2008). However, there are very few studies that assess the toxicological potential of SiC NPs. Recently, it was observed *in vitro* that SiC NPs produce cytotoxicity and genotoxicity on various cell types (Barillet et al., 2010a, 2010b). To the best of our knowledge the toxicological implications and biodistribution of SiC NPs in an *in vivo* rat model have not been evaluated for oral administration. For *in vivo* nanotoxicity assessments, the gastrointestinal (GI) tract is considered to be a major portal of entry for NMs into the organism (Oberdörster et al., 2005a). In fact, NMs can either be ingested or they may inadvertently reach the GI tract after clearance from the respiratory tract through the mucociliary clearance mechanism (Brown et al., 2002; Oberdörster et al., 2005a). The aim of the present study is to assess the biodistribution, toxicity, and elemental composition changes in feces and organs of silicon carbide nanoparticles (SiC NPs) in an *in vivo* rat model after acute (24 h) and subacute (28 days) oral administrations.

* Corresponding author at: University of Namur, 61 rue de Bruxelles, Namur, 5000, Belgium.
E-mail address: omar.lozanogarcia@fundp.ac.be (O. Lozano).
[1] Both authors have participated equally in the study reported here.

0041-008X/$ – see front matter © 2012 Elsevier Inc. All rights reserved.
doi:10.1016/j.taap.2012.08.004

Materials and methods

Nanoparticle dispersions

The NM, SiC NPs, was obtained from Io-Li-Tec (Germany) and used without further treatment. No trace of endotoxin was found using the endotoxin Limulus Amebocyte Lysate kit (Lonza, Switzerland). A SiC NP stock dispersion (100 $mg \cdot mL^{-1}$) was prepared each week with tap water, stirred for 30 min and stored at 4 °C before use. Fresh dilutions were prepared from the stock solution every day at selected concentrations for either the acute or subacute assessments. The choice of dispersing SiC NPs with regular water rather than ultrapure water was to mimic a real life scenario of NP exposure. The lack of use of a surfactant, like Pluronic F108, was decided in order to avoid surface and particle size distribution modifications (Mejia et al., 2012; Taurozzi et al., 2011). It should be noted that throughout this manuscript any mention of SiC implies NPs of SiC, unless otherwise specified.

Nanoparticle characterization

The particle size distribution of pristine SiC was characterized with a Transmission Electron Microscope (TEM) Tecnai 10 Philips at 80 kV. A droplet (10 μl, concentration: 1 $mg \cdot ml^{-1}$) was left to dry on a copper grid covered with formvar.

Particle size distributions (PSD) (in number and weight) were measured with a disk centrifuge DC24000 system (CPS instruments Inc., USA). This measurement is based on the centrifugal liquid sedimentation (CLS) method according to Stokes' law using a 405 nm wavelength laser. This method is also known as Differential Centrifugal Sedimentation (DCS) or ultracentrifugation. The diameters measured are hydrodynamic diameters, which for spherical particles provide the real diameter (sphericity factor equal to 1). A certified calibration standard of PVC microparticles (226 nm), provided by CPS Instruments, was used to calibrate all the measurements. Each measurement was done by injecting 0.1 ml of the stock dispersion into the centrifugal disk (see Nanoparticle dispersions for details).

Specific surface area measurements were obtained by the BET method with an Accelerated Surface Area and Porosimetry System (ASAP, Micromeritics 2010).

Surface composition was analyzed with an X-ray Photoelectron Spectroscopy (XPS) system. The apparatus used is an SSX-100 system using Al K-α X-rays, with spectra recorded at 35° take-off angle. The analysis depth of XPS is around 5 nm. Core-level lines (C1s, Si2p) were calibrated to the C1s peak (284.6 eV) and Au4$f_{7/2}$ peak (84.0 eV). The spectra were analyzed, fitting the Gaussian function to the experimental curve, with a non-linear least squares scheme, and using a Shirley background. Nominal resolution was measured as full width at half maximum of 1.0 eV (core-level spectrum) to 1.5 eV (survey spectrum). Pristine SiC was deposited as such on a gold slab, while a droplet of the stock dispersion was left to dry on the gold slab (see Nanoparticle dispersions for details).

Oral administration protocol

Animals. Female Sprague–Dawley rats (Charles River, France), were used for acute oral toxicity studies (age: 8 weeks, weight: 190–200 g) and for subacute oral toxicity studies (age: 6 weeks, weight: 150–170 g). The animals were housed in a controlled environment at a temperature of 20–22 °C, humidity of 45–65%, and 12 h light/dark cycle. They had free access to tap water and to commercial laboratory complete food (SAFE (Scientific Animal Food & Engineering), rats and mice. Product #A03-10, batch 12037, Belgium). After acclimatizing, the animals were housed in individual type III cages or in metabolic cages (Techniplast COD.170013, Belgium). A daily monitoring of stress, morbidity and mortality was performed. All animal experiments were done in agreement with the local ethics committee for animals. Each dose was administered between 9 and 10 am, feces and urine were collected between 8 and 9 am.

Acute exposure. To evaluate the potential acute oral toxicity of SiC, the OECD (Organization for Economic Cooperation and Development) guideline 420 for acute toxicity study of chemicals was used as a reference (OECD, 2001). The recommended doses in this guideline had to be adapted for NPs due to technical limitations. For example, the highest recommended dose for acute oral toxicity is 2000 $mg \cdot kg^{-1}$, nevertheless, such high concentration of NPs agglomerates and sediments in aqueous media due to the NPs' physicochemical properties (Bagwe et al., 2006; Mejia et al., 2012). The maximal dose found to avoid sedimentation was 600 $mg \cdot kg^{-1}$.

The administration of SiC was performed in a sequential scheme adapted from the predetermined dose method (OECD, 2001). The lowest single dose of SiC dispersion was administered to the first group of rats. The administration of a higher dose to the next group was done 24 h later. If at least one animal of the group should die or show any sign of external or visual toxicity, the NPs at that concentration are considered toxic and subsequent higher doses are not administered.

Homogeneous SiC dispersions were freshly prepared every day using tap water, and stirred during 30 min. The concentrations were prepared at 0.1, 1, 10, 60 and 120 $mg \cdot mL^{-1}$ and were administered at doses of 0.5, 5, 50, 300 and 600 $mg \cdot kg^{-1}$, respectively, respecting a dose volume of 5 $mL \cdot kg^{-1}$. The dispersions were administered orally with a rigid stainless steel needle. The rats were divided in 6 groups of five rats per group: a control group which received only tap water whereas the 5 other groups received the SiC dispersions. Each group was divided in 2 sub-groups: 2 rats in conventional type III cages and 3 rats individually housed in metabolic cages. The rats were observed at 10 and 30 min, 18 and 24 h after NP administration. Afterwards, they were sacrificed by intraperitoneal injection of Nembutal (60 $mg \cdot kg^{-1}$), followed by an autopsy.

Subacute exposure. To evaluate the potential subacute toxicity of SiC, OECD guideline 407 for chemicals for subacute toxicity of chemicals was used as a reference (OECD, 1995). Fresh dilutions from the SiC stock solution were prepared every day at concentrations of 0.1 $mg \cdot mL^{-1}$ and 10 $mg \cdot mL^{-1}$ to be administered at 0.5 $mg \cdot kg^{-1}$ and 50 $mg \cdot kg^{-1}$ to the animals. The dispersions were administered orally to rats using a rigid stainless steel needle. Administration was performed once per day, five days per week and during 4 consecutive weeks (28 days). These low and mild doses were selected due to their periodic administration, based on the results obtained from the acute toxicity study. The total administered dose at the end of the assessment was 10 $mg \cdot kg^{-1}$ and 1000 $mg \cdot kg^{-1}$.

The rats were divided in 3 groups of six rats per group: a control group receiving only tap water, a group receiving the low dose (0.5 $mg \cdot kg^{-1}$) and a group receiving the high dose (50 $mg \cdot kg^{-1}$). Each group was divided in 2 sub-groups for the individual housing: 3 rats in conventional type III cages and 3 rats in metabolic cages. Rats were acclimatized to the environment during 2 weeks before the oral administration assessments. The rats were observed at 10 and 30 min, 18 and 24 h after oral administration. Rats were sacrificed at the end of the 28 days by an intraperitoneal injection of Nembutal (60 $mg \cdot kg^{-1}$) and autopsy was performed afterwards.

Detection of SiC and elemental composition analysis on feces and organs

Sample preparation. Feces were collected on a 24 h basis: every 24 h for the control rats, every 24 h after acute exposure, or every 24 h just before the next dose administration for the subacute exposure. The dose (or first dose in subacute exposure) was applied on day 0. This means that, for example, the values reported for day 1 correspond to the collected feces produced during the prior day. Several organs were studied by PIXE after acute exposure: the liver, kidneys and spleen.

Both feces and organs were prepared into pellets for ion beam analysis. The feces were dried in an oven at 60 °C for 24 h. The daily amount of rat feces allowed the preparation of up to 3 pellets per rat, all of them were measured and averaged. Each pellet of feces was prepared with the following procedure: feces were weighed and then chromium nitride (Cr_2N) powder (Goodfellow, 99% purity, 45 μm particle size) was added in a ratio of 7–10% of the feces weight. Both feces and Cr_2N powder were then subjected to ball milling in order to get a homogeneous powder mixture. This mixture was finally hard pressed into a pellet (diameter: 2 cm, thickness: 1 mm). In the case of organs, they were dried in an oven at 37 °C for 24 h, and then weighed. Organs were dry-frozen with liquid nitrogen (Galuszka et al., 1984), powdered by ball milling with 7–10% of Cr_2N powder, and then hard pressed to produce pellets (diameter: 2 cm, thickness: 1 mm). The reason for mixing feces or organs with Cr_2N is to avoid charge accumulation during ion beam analysis in the sample, and to use Cr as an internal standard for quantitative measurements (Lozano et al., 2012). Chromium was selected because it is not present in the biological matter, nor as an impurity in SiC, and it does not interfere with other elements during the PIXE measurements.

PIXE analysis. Ion beam measurements were performed with the ALTAÏS accelerator of the University of Namur. The incident ion beam was 2 MeV protons, and both Particle-Induced X-ray Emission (PIXE) and Rutherford Back-Scattering (RBS) measurements were done simultaneously. The geometry and setup for the measurements have been described previously (Lozano et al., 2012). Briefly, with respect to the beam direction: the sample was tilted at 45°, a Canberra LEGe (Low Energy Germanium) detector was located at 90° for PIXE measurements, and a Canberra PIPS detector was positioned at 145° for RBS measurements. An aluminum collimator with a 3 mm aperture was used in front of the PIXE detector. The samples were mounted on a rotating device which provided a total scan area of 140.5 mm^2.

PIXE measurements were validated with two standards from the International Atomic Energy Agency (IAEA 153 and IAEA 155). The results are in agreement with respect to the reported values (better than 5%) (IAEA, 1989; IAEA, 1990). The addition of 7–10 wt.% of Cr_2N to the samples was chosen as a best compromise between the X-ray yield from the biological material and SiC with respect to the X-ray attenuation caused by a heavy-element inclusion into the matrix (biological matter). Data analysis included this attenuation factor. A 2 MeV proton beam has a penetration depth of 43.81 μm to 42.15 μm into a biological matrix containing 7% to 10% Cr, respectively. Therefore, small variations in the amount of Cr_2N powder into the biological matrix have less than 5% change in the measured volume per sample. For a biological matrix under similar analysis conditions the limit of detection (LOD) of Si is 40 ppm (Lozano et al., 2012), and thus the limit of quantification (LOQ) is 133 ppm. Other elements have been measured in either feces or organs: magnesium (Mg), phosphorous (P), sulfur (S), chlorine (Cl), potassium (K), and calcium (Ca). Their respective LOD and LOQ are presented as element (LOD, LOQ) in ppm: Mg (87, 290), P (32, 107), S (24, 80), Cl (19, 63), K (16, 53), and Ca (60, 200).

Statistical analysis. All the biodistribution data was analyzed using the Holm–Sidak method (two way ANOVA). The statistical significance was compared between the control and dosed samples, dosed samples, and control samples; dividing the significant results in $p<0.05$, $p<0.01$, and $p<0.001$.

Detection of SiC in urine

Urine samples were collected from each rat every day during the experiment. Afterwards a filtration procedure and urine samples were analyzed with a Jeol FEG-SEM operated at 20 keV with an EDX (Energy Dispersive X-ray) detector. The filtration procedure was the following: a fraction of the urine (2 mL) was deposited on a 650 nm filter inside an ultrafree centrifugal filter (Millipore, USA) and centrifuged at 10,000 *g* during 2 min. Then the filtrate was collected and deposited on a 450 nm filter inside an ultrafree centrifugal filter, and submitted to centrifugation at 10,000 *g* during 2 min. Afterwards, the filtrate obtained was deposited on a 220 nm filter inside an ultrafree centrifugal filter, and submitted once more to centrifugation at 10,000 *g* during 2 min. Finally, the filtrate obtained was deposited on a 100 nm filter inside an ultrafree centrifugal filter, and submitted once more to centrifugation at 10,000 *g* during 2 min. The filters of 220 and 450 nm were prepared for FEG-SEM observation. 500 μL of 2.5% glutaraldehyde in 0.1 M cacodylate buffer (composed of $Na(CH_3)_2 \cdot AsO_2 \cdot 3H_2O$ in distilled water at pH 7.4) was placed on the filter for 1 h. The glutaraldehyde solution was removed by centrifugation at 10,000 *g* during 2 min, then 500 μL of 0.2 M cacodylate buffer was added. Filters were washed with 0.2 M cacodylate buffer. The next step was the dehydration of the sample with successive baths of alcohol from 30 to 100 °C. A critical drying point was performed with a Balzers Critical Point Dryer (CPD) 030 (BAL-TEC Gmbh®, Germany). Afterwards, a thin layer of platinum (20 nm) was deposited under argon on filters with the metallizer Balzers union (BAL-TEC Gmbh, Germany).

Toxicity assessment

Morphological and pathological examinations. Organs (esophagus, stomach, intestines, bladder, spleen, pancreas, kidneys and liver) were collected during the autopsy. The liver, kidneys and spleen were weighed. All organs were fixed in formaline 10%, embedded in paraffin blocks and cut into slices (6 μm thick). The sections were placed on glass slides, and revealed by a staining technique using hematoxylin and eosin (H&E). The slides were observed under an optical microscope (Olympus Provis AX70). Micrographs were taken with a camera (Zeiss AxioCam). Histological sections were made in the esophagus, stomach, small intestine, large intestine, bladder, spleen, liver and kidneys. Histopathological examination was conducted in collaboration with the Institute of Pathology and Genetics (IPG, Gosselies, Belgium).

Plasma analysis. Blood samples from the left ventricle of the heart were stored for all animals per group ($n=6$), using a 21-gauge needle and collected in heparin and citrated tubes. Plasma was obtained after centrifugation at 2000 *g* for 10 min. Potassium, glucose, total cholesterol, PA and albumin were analyzed. Parameters reflecting the liver function as ASAT and ALAT and reflecting the renal function as urea and creatinine were also measured at the clinical biology laboratory of CHU (Sart Tilman — Ulg, Belgium) using a COBAS® 6000 (Roche, USA). Bile salts were analyzed at the Laboratory of Dr Collard (Liège, Belgium) using an Architect C8000 (ABBOTT, Belgium).

Urine analysis. Urine parameters were analyzed: urinary osmolarity was determined after a twofold dilution in ultrapure water (milliQ 18.2 MΩ·cm) with a micro-osmometer (Fiske Micro-osmometer Model 2010, USA). The concentrations of sodium and potassium were measured in urine samples after a twofold dilution in ultrapure water (milliQ 18.2 MΩ·cm) with an Instrumentation Laboratory 943 (Instrumentation Laboratory).

Statistical analysis. All the toxicity assessment data were analyzed with GraphPad Prism software using a non-parametric Mann–Whitney test by comparing the control and treated samples.

Results

Nanoparticle and dispersion characterization

A TEM image of SiC is shown in Fig. 1. The observed average diameter is 36.2 ± 8.6 nm. The specific surface area, the surface that

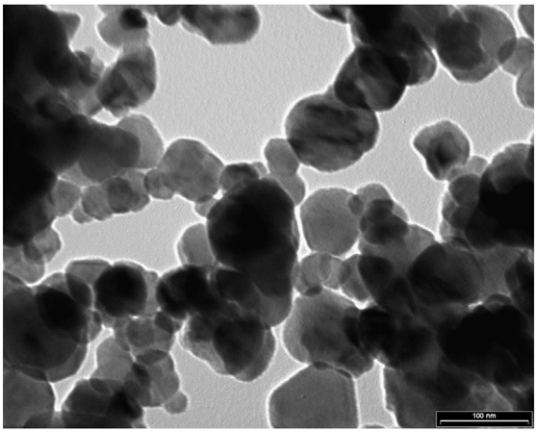

Fig. 1. TEM image of pristine SiC. The average diameter is 36.2 ± 8.6 nm. Scale bar: 100 nm.

can potentially interact with the external media (dispersant media, biomolecules and/or biological systems), was measured as 30 $m^2 \cdot g^{-1}$.

The CLS results, PSD in weight and number, are presented in Fig. 2 for the SiC dispersion. Each figure represents different PSD information from the same dispersion. The particle number distribution (Fig. 2b) is composed of two sub-distributions, primary (individualized) particles and aggregates. SiC primary particles have an average hydrodynamic diameter of 23 nm with a full width at half maximum of 21–33 nm. Thus, the primary particles (<70 nm) constitute 57% of the dispersion, with the remaining 43% as aggregates. The PSD weight of the SiC dispersion (Fig. 2a) shows a single distribution with a hydrodynamic diameter of 350 nm. Using the cutoff hydrodynamic diameter of the primary particles, found as 70 nm (Fig. 2b), those represent only 0.26% of the product in terms of weight, while the rest (99.74%) are aggregates.

Fig. 3 presents the XPS results of pristine and dispersed SiC. No contaminants were found in the surface. Figs. 3a and b show the Si and C regions from pristine SiC, respectively, with their identified compound contributions (Shimoda et al., 2007; Taylor, 1989): the Si region presents compounds of SiC, SiO_2 and Si; while the C region shows C–C, SiC, and Si oxycarbide compounds. The Si and C regions for the dispersed SiC are presented in Figs. 3c and d, respectively: the Si region shows a complete absence of pure Si and in addition to the SiC and SiO_2 compound there is a clear Si oxycarbide component in the region (Shimoda et al., 2007); and the C region presents the appearance of CO compounds along with C and Si oxycarbide (SiC_xO_y) compounds (Shimoda et al., 2007). The surface composition of pristine and dispersed SiC is summarized in Table 1, where the dispersed SiC composition shows a reduced amount of Si and an increased amount of C.

Elimination of SiC via feces excretion, elemental composition of feces and organs

Rat food analysis. PIXE was used to quantify the trace elements in the food ingested by rats. Table 2 shows that Si is one of the traces present in the food. The estimated food eaten per rat per day was 16.9 g, accounting for an average of 22.44 mg of ingested Si per day. The low and high doses, in the subacute assessment, were administered as a function of the rat weight (182 g at day 1 and increased on average to 244 g at day 28), and thus the orally administered low and high doses ranged between 0.091–0.122 mg and 9.1–12.2 mg for the 0.5 and 50 mg/kg doses at day 1 and day 28, respectively. Therefore only the high dose group (50 mg/kg) can be measured by differentiating it from the ingested Si in the food.

Feces analysis: subacute exposure. Feces from selected days were analyzed by PIXE in order to evaluate their SiC content following subacute oral administration. The SiC content was evaluated from the Si signal (see Fig. 4a). All the feces of each selected day (control and SiC exposed groups) were analyzed. Data from the SiC exposed group were normalized with the data from the control group from the same selected day. Additionally, the data were normalized with respect to the average rat weight of the selected day to account for the increase of dosed SiC with an increased weight. During the period of the exposure the data seems to fit a linear increasing trend, except during the weekend where the excreted Si decreases close to the values of the control group, indicating the fast elimination of SiC when rats are not subjected to SiC doses. There is a statistically significant increase of 45% of the excreted Si during the full term of the subacute study. In

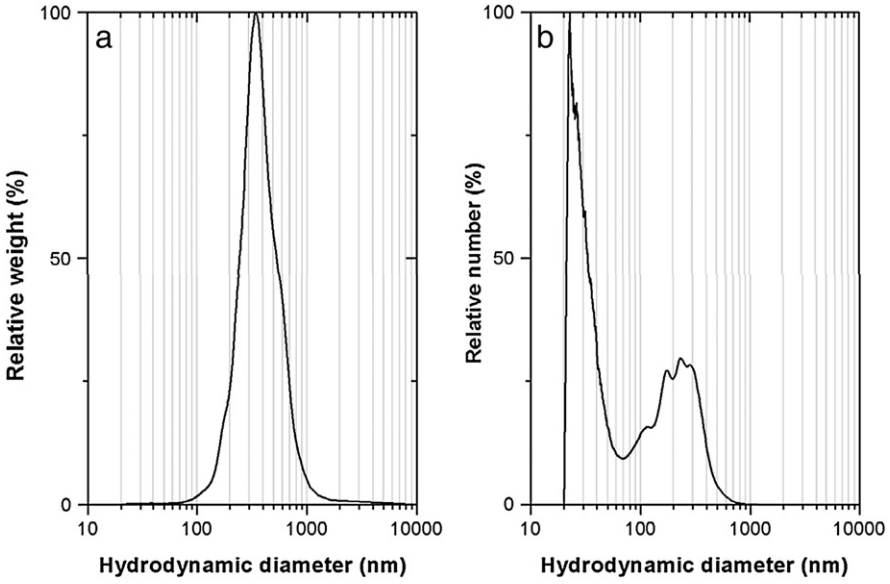

Fig. 2. CLS particle size distribution: (a) weight relative distribution and (b) number relative distributions for SiC dispersed in tap water and agitated for 30 min. The weight relative distribution shows that most of the dispersed SiC is composed of aggregates, while the number relative distribution indicates the quantity of primary particles is similar to the amount of aggregates.

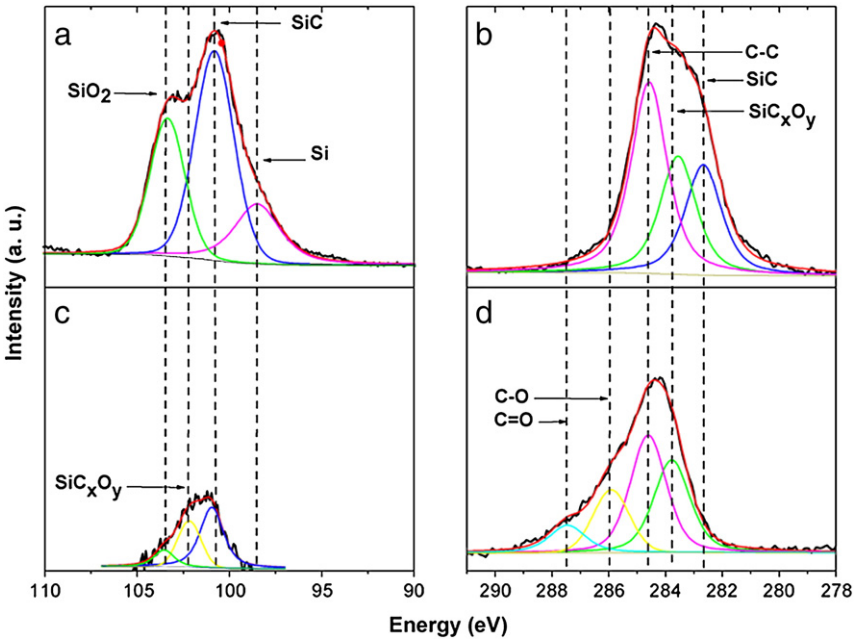

Fig. 3. XPS spectra regions of SiC: (a) Si region of pristine SiC, (b) C region of pristine SiC, (c) Si region of dispersed SiC, and (d) C region of dispersed SiC. Each peak was identified with respect to a specific chemical bond.

addition to Si, other elements were quantified such as Ca, P, and Mg. A statistically significant increase of these elements was also found in the excreted feces from SiC exposed rats during the full term of the subacute study, see Figs. 4b–d, accounting for 29, 18, and 39% for Ca, P, and Mg, respectively. Table 3 summarizes the absolute values of the control and treated groups.

Feces analysis: acute exposure. Feces from rats subjected to an acute oral administration were analyzed in order to clarify the rate of excreted SiC. Fig. 5a shows the amount of Si excreted from days one to three. The normalization procedure was the same applied to the subacute assessment. An extrapolation of the decrease rate indicates that SiC would be completely excreted on day 5. The amount of excreted SiC on day one accounts for 67% of the total excreted feces, the rest is excreted in subsequent days. Other elements were measured and only K showed a statistically significant difference in the studied time range, see Fig. 5b, presenting an oscillating value close to 60% higher than the control value. Table 4 summarizes the absolute values of the control and treated groups.

Organ analysis: acute exposure. Several organs were prepared for element analyses by PIXE: liver, kidneys, and spleen. The rats were given a single dose of SiC by oral administration and were sacrificed one or seven days later. Fig. 6 summarizes the organ elemental analyses using PIXE. Data were normalized with respect to their control values. No trace of Si was observed in any of these organs, indicating that if SiC could pass through the intestinal barrier either it was quickly excreted in urine or only trace amounts can pass at levels below the limit of detection of the technique. The other studied elements are presented in Figs. 6a–c for liver, kidneys, and spleen, respectively. All the organs present small statistically significant variations in several elements. The liver presents an increase of P, S, Cl, and K on day one and a decrease of the same elements towards day seven. A steep decrease of Ca is also observed in the liver on day one and remains lower than the control values towards day seven. Both kidneys and spleen present a qualitative similar behavior: there is a decrease on day one for P, S, Cl, and K and on day seven an increase is observed. This is contrary to the response of the liver. Table 5 summarizes the absolute values of the control and treated groups.

Elimination of SiC by urine excretion

Urine samples, from the subacute assessment, were observed by electron microscopy (FEG-SEM) after a filtration and centrifugation process in order to detect the possible presence of SiC in urine. A sample image from the urine of a SiC exposed rat is shown in Fig. 7 with the 200 nm filter. Trace amounts of granular agglomerations were found only in the urine of SiC exposed rats. The analysis with EDX, see Fig. 7, indicated that these agglomerations exhibit a strong Si signal, thus qualitatively confirming that SiC can pass the intestinal barrier. No granular agglomerations were found in the 100 nm filters, suggesting that SiC traces in urine were concentrated in the 200 nm filters.

Table 1
The surface composition of SiC in pristine and dispersed conditions using XPS.

Nanoparticle	Element (at.%)		
	Si	C	O
SiC (pristine)	36.9	26.9	36.2
SiC (water dispersed)	22.2	44	33.8

Table 2
Trace impurities present in rat food using PIXE.

Element	Trace element concentration (ppm)
P	9483
K	4439
Cl	3719
Ca	4693
Si	1328
S	2884
Ti	666
Fe	591
Cu	427

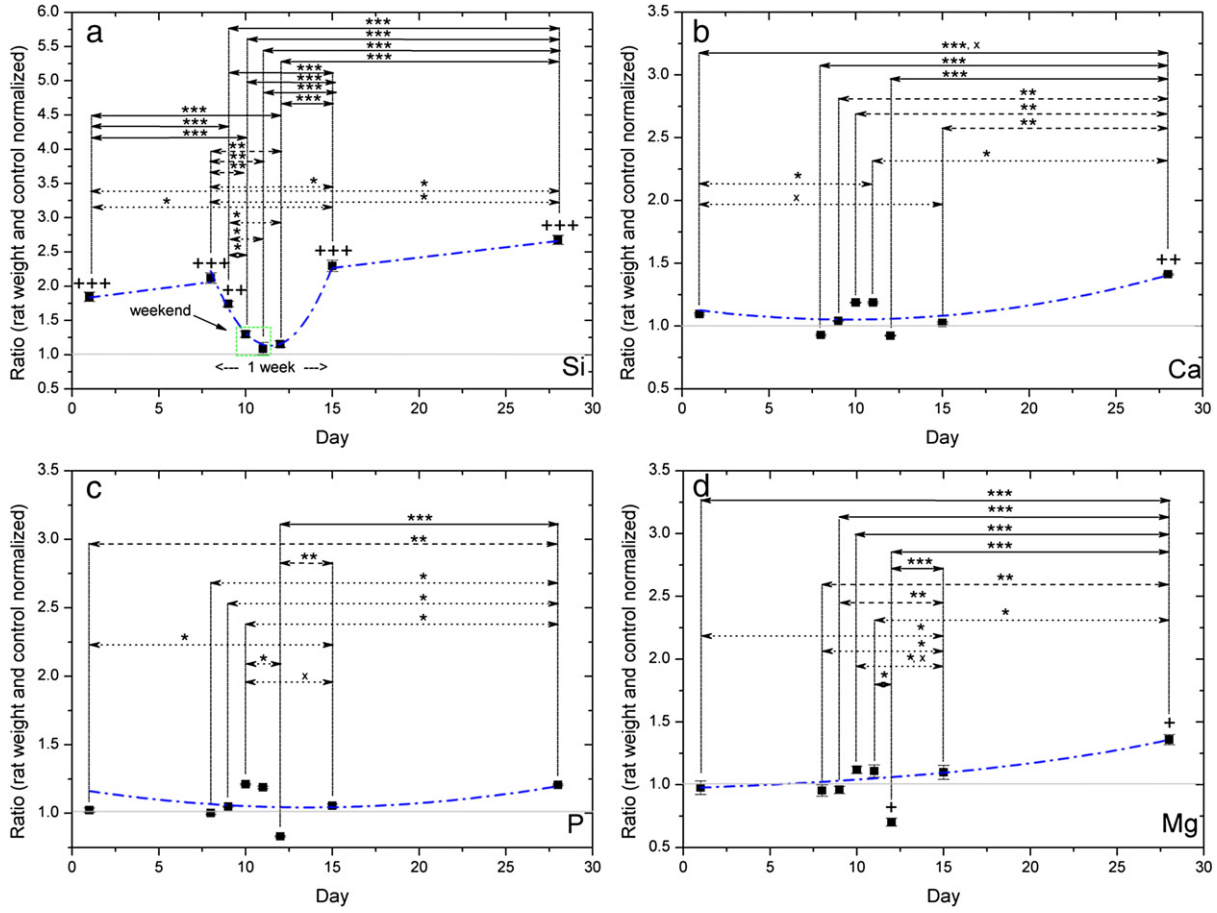

Fig. 4. PIXE analyses of rat feces during subacute administration of 50 $mg \cdot kg^{-1} \cdot day^{-1}$ of SiC from selected days. SiC administration was done only during weekdays. All plots have been normalized with respect to rat weight and control values. Variation of: (a) Si, (b) Ca, (c) P, and (d) Mg. Statistical analysis: two way ANOVA using the Holm–Sidak method. Statistical significance between: control and dosed samples (+), dosed samples (*), control samples (x). +, *, x indicates $p<0.05$; ++, **, xx indicates $p<0.01$; +++, ***, xxx indicates $p<0.001$. The dashed-dot lines (— · —) are guides to the eye.

Acute toxicity

The animals received a single dose of SiC (0.5, 5, 50, 300 or 600 $mg \cdot kg^{-1}$) dispersed in tap water using a stainless steel needle. All the animals survived the single administration of SiC, regardless of the concentration, and did not show any sign of discomfort (lethargy, nausea, vomiting or diarrhea) during the 24 h following SiC administration.

Table 3
Summary of rat feces elemental quantification from PIXE analysis of control and treated groups from the subacute exposure study.

Day on study	Weight (g, mean ± SD)	Fecal mass collected (mg)	Elemental analysis (ppm)			
			Si	Ca	P	Mg
Control group						
1	194.67 ± 13.58	1572	8720 ± 499	62,792 ± 378	81,196 ± 1182	68,622 ± 2376
8	208 ± 5.57	1931	7281 ± 500	80,733 ± 453	89,630 ± 598	72,673 ± 2446
9	210 ± 7.57	1709	7328 ± 254	82,387 ± 255	84,082 ± 307	62,647 ± 1189
10	214 ± 12.12	1548	6786 ± 238	79,618 ± 251	77,352 ± 289	55,315 ± 1101
11	217.67 ± 8.14	1763	8040 ± 503	80,330 ± 446	88,622 ± 581	69,361 ± 2365
12	219.71 ± 5.57	1694	7752 ± 292	86,197 ± 303	90,381 ± 377	73,858 ± 1663
15	226 ± 11.36	2114	8811 ± 610	91,332 ± 517	108,318 ± 742	81,112 ± 2966
28	256.33 ± 6.11	1651	7561 ± 441	94,941 ± 384	104,859 ± 508	76,022 ± 2151
Treated group						
1	188.33 ± 9.29	1505	15,574 ± 598	66,565 ± 428	80,394 ± 623	64,892 ± 2630
8	203.67 ± 13.65	1958	15,110 ± 495	73,424 ± 380	87,931 ± 519	67,859 ± 2113
9	209 ± 14.29	1729	12,704 ± 280	85,294 ± 276	87,803 ± 332	59,843 ± 1271
10	211 ± 14.98	1842	8699 ± 270	93,173 ± 279	92,412 ± 333	61,020 ± 1222
11	219 ± 13.11	2131	8802 ± 571	95,967 ± 520	106,012 ± 681	77,411 ± 2648
12	216.16 ± 15.31	1778	8803 ± 240	78,283 ± 260	73,914 ± 306	51,058 ± 1112
15	228.33 ± 20.31	2180	20,452 ± 866	94,682 ± 630	115,510 ± 921	90,068 ± 3739
28	254.67 ± 16.65	1558	20,106 ± 627	133,283 ± 527	125,814 ± 590	102,583 ± 2976

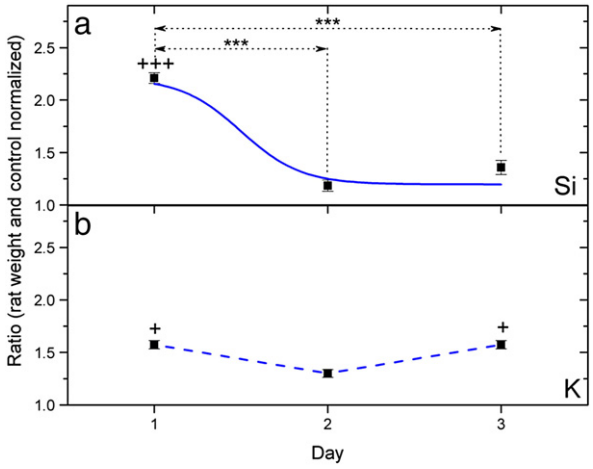

Fig. 5. PIXE analysis of rat feces with acute administration of 50 mg·kg^{-1} of SiC, at selected days. All plots have been normalized with respect to rat weight and control values. (a) Variation of Si. (b) Variation of K (note: $p<0.05$ when comparing all dosed samples *versus* all control samples). Statistical analysis: two way ANOVA using the Holm–Sidak method. Statistical significance between: control and dosed samples (+), dosed samples (*), control samples (x). +, *, x indicates $p<0.05$; ++, **, xx indicates $p<0.01$; +++, ***, xxx indicates $p<0.001$. The dashed-dot lines (— · —) are guides to the eye.

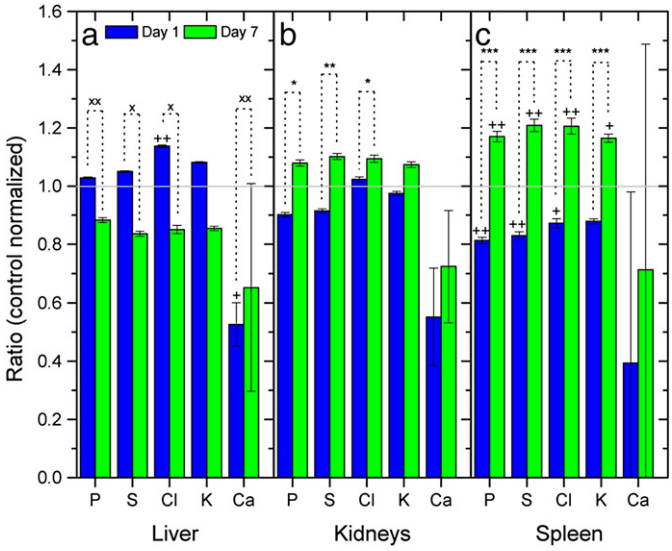

Fig. 6. PIXE analysis of element variation in different rat organs at one day and seven days after acute administration of 50 mg·kg^{-1} of SiC. All plots have been normalized with respect to rat weight and control values. (a) Liver, (b) kidneys, and (c) spleen. Statistical analysis: two way ANOVA using the Holm–Sidak method. Statistical significance between: control and dosed samples (+), dosed samples (*), control samples (x). +, *, x indicates $p<0.05$; ++, **, xx indicates $p<0.01$; +++, ***, xxx indicates $p<0.001$.

Twenty four hours after the administration, all the animals were submitted to a detailed autopsy. From a macroscopic point of view, no change was observed in the organs from the GI tract (stomach, intestines and colon), nor in the liver, spleen, kidneys or bladder.

Several blood parameters were measured: potassium, glucose, total cholesterol, PA, albumin, parameters reflecting the liver function (TGO and TGP), bile salts and parameters reflecting the kidney function such as urea and creatinine. No difference was observed between the control and treated animals and all the studied parameters were found in the normal range of values described for rats (data not shown) (Krinke et al., 2000).

Histopathological examinations showed that the stomach and intestines were not affected by the administration of SiC NPs (see Appendix A). The epithelium of target organs (stomach, small and large intestines) of the GI tract did not exhibit irregularities, even at the dose of 600 mg·kg^{-1}. SiC NPs can be observed in the stomach lumen of the animals only after the administration of the highest dose (600 mg·kg^{-1}) (Fig. 8).

The kidney examination of the control and SiC exposed groups is shown in Fig. 9. No anomalies were observed between the control and exposed groups: the medullar and the cortex exhibited a normal aspect. This indicates that no renal damage has occurred within the 24 h following SiC administration.

Table 4
Summary of rat feces elemental quantification from PIXE analysis of control and treated groups from the acute exposure study.

Day on study	Weight (g, mean ± SD)	Fecal mass collected (mg)	Elemental analysis (ppm)	
			Si	K
Control group				
1	168 ± 6.25	2065	5912 ± 263	2318 ± 73
2	166.67 ± 3.51	2280	5927 ± 197	2187 ± 52
3	169.83 ± 9.17	2495	5943 ± 293	2315 ± 71
Treated group				
1	163 ± 3.21	2658	12,673 ± 331	3540 ± 90
2	164.33 ± 5.03	1864	6925 ± 292	2804 ± 78
3	167.33 ± 4.72	2518	7242 ± 288	4455 ± 84

The histopathological examination of the liver showed that the architecture of the liver was not affected by SiC administration (Fig. 10). Granulomas were found in the liver parenchyma of both the SiC treated and control groups with no significant difference between both groups (Table 6). In laboratory animals under conventional housing, granulomas are common spontaneous lesions in the liver (Greaves, 2007). They have numerous causes (drugs, bacterial, fungal, parasitic or viral infections, liver or systemic disorders) and are usually asymptomatic (Shiga et al., 2010). Given that this work was not performed under SPF (Specific Pathogen Free) conditions and that liver granulomas were also observed in control animals without a significant difference, it is not

Table 5
Summary of rat organ elemental quantification from PIXE analysis of control and treated at one day and seven from the acute exposure study.

Organ	Elemental analysis (ppm)				
	P	S	Cl	K	Ca
Control group (24 h)					
Liver	10,550 ± 22	6852 ± 14	2611 ± 9	7868 ± 14	270 ± 10
Kidneys	9636 ± 51	6463 ± 33	4078 ± 24	5627 ± 26	169 ± 15
Spleen	10,268 ± 85	5202 ± 49	2910 ± 34	7922 ± 50	170 ± 54
Treated group (24 h)					
Liver	10,855 ± 20	7196 ± 13	2970 ± 9	8511 ± 13	142 ± 9
Kidneys	8693 ± 42	5914 ± 28	4174 ± 21	5487 ± 23	93 ± 13
Spleen	8349 ± 66	4318 ± 39	2539 ± 28	6964 ± 41	66 ± 32
Control group (7 days)					
Liver	15,344 ± 85	9400 ± 53	3351 ± 32	8688 ± 42	128 ± 27
Kidneys	11,037 ± 87	7255 ± 56	4683 ± 42	6227 ± 44	206 ± 25
Spleen	11,090 ± 155	5225 ± 86	2833 ± 61	8375 ± 90	96 ± 46
Treated group (7 days)					
Liver	13,553 ± 82	7861 ± 50	2851 ± 30	7425 ± 41	84 ± 24
Kidneys	11,911 ± 87	7993 ± 57	5123 ± 42	6684 ± 43	149 ± 22
Spleen	12,981 ± 149	6317 ± 85	3416 ± 59	9754 ± 88	68 ± 42

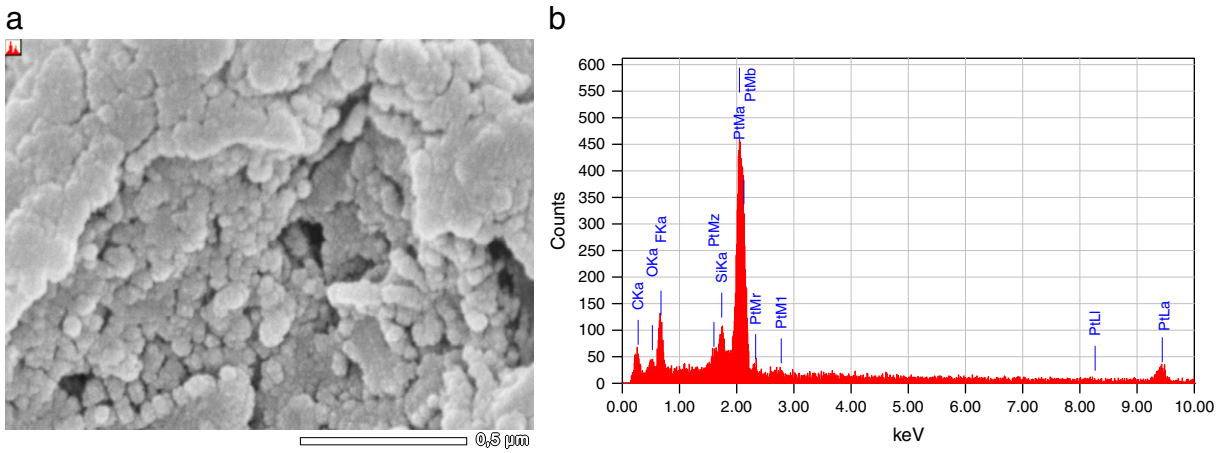

Fig. 7. FEG-SEM image of SiC in the urine filtered through a 220 nm mesh from 50 mg·kg^{-1} treated rats at the 28th day of experiment. EDX spectrum shows the signal of Si, indicating the presence of SiC.

possible to conclude on the toxicological relevance of these hepatic granulomas after administration of SiC NPs.

Subacute toxicity

The subacute toxicity study (28 days) was performed with SiC dispersions administered orally at a concentration of 0.5 or 50 mg·kg^{-1} during five days a week, for four weeks.

The rats were observed after 10 and 30 min, 18 and 24 h after each administration and their behavior was evaluated. Each animal survived the treatment with SiC on both concentrations, and did not show any sign of discomfort (lethargy, nausea, vomiting or diarrhea) during the whole experiment. The animals were weighed every day during the experiment, no abnormal weight variations were observed during this period. At the end of the experiment, the animals weighed between 250 and 300 g which corresponded to normal values of Sprague–Dawley rats of eleven weeks (Krinke et al., 2000). Food and water consumption were also quantified. No change in both consumptions was observed during the 28 days of experiment. On average, animals consumed 79 g/kg of food and 108 mL/kg of water daily. These values were within the physiological reference values for rats (Krinke et al., 2000). Twenty eight days after the first administration of SiC, each animal was submitted to a detailed autopsy. No change was observed on the GI tract organs, liver, spleen, kidneys and bladder from a macroscopic point of view. There was no significant difference in the organs' weight between the control and the SiC exposed groups.

Histopathological analyses of different organs (esophagus, stomach, intestines, liver, kidney, bladder and spleen) were performed. The histopathological examination of the GI tract (esophagus, stomach, and intestines) showed no differences between the control group and the SiC exposed groups (see Appendix A). Similarly, kidney (renal cortex) or liver (parenchyma) was without anomalies for the SiC treated rats (see Appendix A).

Histological sections of the liver were used to quantify the number of granulomas. The control group presented a density of 0.65 ± 0.36 granulomas·cm^{-2}, which is similar to the density found in the low dose group; while the high dose group presented an increase to 1.03 ± 0.95 granulomas·cm^{-2}, although not statistically significant.

Twenty eight days after the first SiC administration, a blood sample was collected from the intracardiac cavity during necropsy. Table 7 shows the summary of the quantified parameters. All the plasmatic parameters measured are in the normal range values described for rats (Krinke et al., 2000), except potassium. A statistical significant decrease of the plasmatic urea was found on the SiC treated rats (50 mg·kg^{-1} group) and suggests a possible liver damage or malabsorption (Mezey, 1982).

Urine samples were collected each day and quantified. The average daily urine volume collected was 53.2 mL·kg^{-1}, this value is within the physiological reference values described for rats (Krinke et al., 2000). No differences were observed in osmolarity, sodium and potassium of urine in both 0.5 and 50 mg·kg^{-1} SiC treated groups compared to the control group, see Fig. 11.

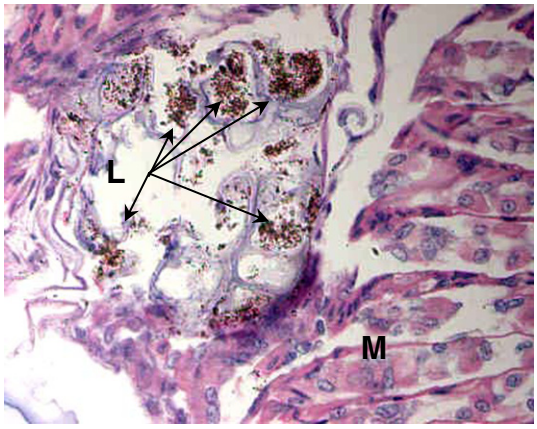

Fig. 8. Histopathological examination of the stomach from a 600 mg·kg^{-1} SiC exposed rat. L, lumen and M, gastric mucosa. Arrows indicated the SiC in the intestinal lumen. H&E, ×400.

Discussion

Physico-chemical properties of SiC

When NMs enter into a biological medium, they are surrounded by proteins and lipids, forming what is known as the hard corona (Lynch and Dawson, 2011; Monopoli et al., 2011; Nel et al., 2009). Thus, the majority of the long term interactions, which could lead to a toxicological response, are mediated between the organism and the NMs' hard corona. Nevertheless, the link between the NMs' properties, hard corona formation and toxicological response is still unclear. There

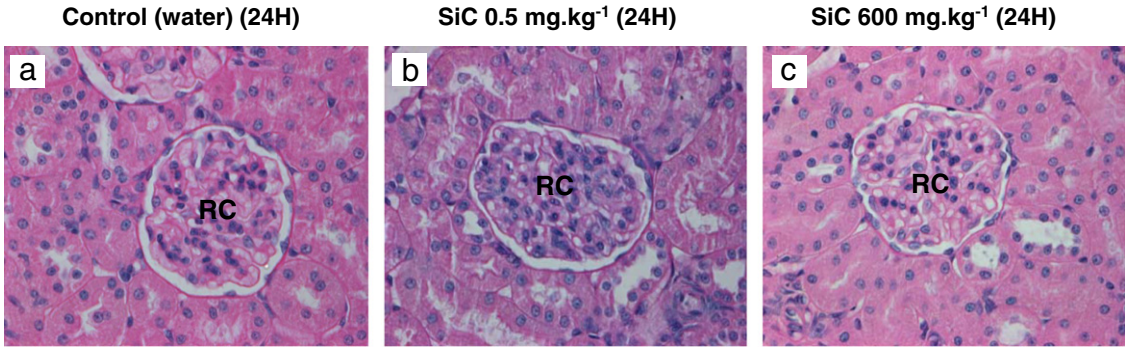

Fig. 9. Histopathological examination of the renal cortex from selected animals. (a) Control group, (b) 0.5 and (c) 600 mg·kg^{-1} SiC exposed groups. RC = renal corpuscles. H&E, ×400.

are some cases where two very similar experiments using similar NMs led to contradictory toxicological results, *i.e.* SWCNT (single-walled carbon nanotubes) (Geraci and Castranova, 2010) or TiO_2 NPs (Churg et al., 1998; Takenaka et al., 1986). The characterization of the pristine and dispersed NMs as thoroughly as possible is therefore necessary in order to follow the evolution of their properties and eventually link these properties to their toxicological response.

The size of pristine SiC assessed by TEM shows clear individual particles with an average diameter of 36.2 ± 8.6 nm. SiC were dispersed in tap water by stirring for 30 min. The selection of a dispersion protocol is not trivial in terms of particle size and surface chemistry (Mejia et al., 2011; Taurozzi et al., 2011). The selection process was made after a scan of several dispersion methods and times (Mejia et al., 2012). Stirring during 30 min is the best condition found allowing a maximum amount of primary particles without deeply altering their surface chemistry with respect to pristine SiC. After dispersion in tap water with 30 min stirring, the majority of SiC agglomerates (held by weak forces: van der Waals) should have been destroyed, leaving only aggregates (held by strong forces: chemical bonds) and primary particles (Oberdörster et al., 2007). From a quantity basis the primary particles (defined up to 70 nm) are 57% and aggregates are 43%. Both primary particles and aggregates seem to be composed of several sub-distributions, and their average hydrodynamic diameter difference is about one order of magnitude of difference: 23 and 230 nm, respectively. A recent study on the fate of SiC when passing through a reconstituted gastric fluid showed that the size of its primary particles increased by 2.7%, and that its proportion increased from 61 to 97%. In that study ultrapure water was used to disperse the NPs. This indicates that some gastric fluid components act as an effective dispersant in SiC, thus incrementing the amount of individualized NPs in the GI tract.

Pristine SiC show that Si bonds with itself, C, and O; and C bonds with C and Si (Shimoda et al., 2007; Taylor, 1989). The surface chemistry of the SiC dispersion shows that Si is completely bonded with either C or O, while the C region bonds with O in addition to C and Si. The change in composition exhibits a reduction of Si and an increase of C, with O being mostly unaltered. The increase in the amount of C is due to contaminants coming from both the environment and from within the SiC agglomerates which are released after stirring (Mejia et al., 2012). This increase in surface C buries the Si atoms deeper, thus showing a decrease in its surface amount. The overall purity of the SiC was assessed with PIXE.

These results show that the NP dispersions administered to the rats are actually a mix of individualized particles and aggregates which have undergone surface chemistry changes in comparison to the pristine product.

Biodistribution of SiC and elemental composition changes to feces and organs

The trace concentration of SiC in feces excretion from the subacute experiment presents a linearly increasing long term and a parabola short term pattern. The short term pattern, over the span of a week, is parabolic with the lowest value measured during the weekend reaching close to control values. This excretion rate is in agreement with the tendency from the subacute experiment. It should be noted that the two values adjacent to the weekend values show a lower excretion of Si than the expected long term pattern. Thus, it is apparent that SiC can remain in the GI tract walls or be absorbed at different rates depending on the frequency of SiC administration. The observed short term pattern should repeat itself during each of the four weeks of exposure, following an incremental tendency as revealed by the long term pattern. For the

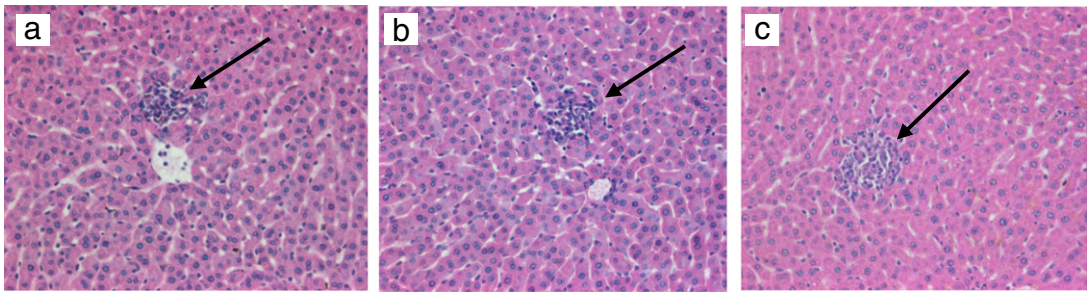

Fig. 10. Histopathological examination of the liver from selected animals. (a) Control group, (b) 0.5 and (c) 600 mg·kg^{-1} SiC exposed groups. Arrows represent granulomas in liver parenchyma. H&E, ×200.

Table 6
Number of granuloma·cm^{-2} in liver histopathological sections. Mean ± SD, n = 5.

Group	Granuloma·cm^{-2}
Control	0.63 ± 0.34
0.5 mg·kg^{-1}	0.84 ± 0.79
5 mg·kg^{-1}	0.36 ± 0.48
50 mg·kg^{-1}	0.14 ± 0.13
300 mg·kg^{-1}	0.81 ± 0.40
600 mg·kg^{-1}	0.48 ± 0.58

Table 7
Plasmatic concentration of SiC-treated groups compared with the control. Mean ± SD, n = 6.
Physiological range from Sharp and La Regina, 1998.

Parameters (physiological range)	Control water	Group 1 0.5 mg·kg^{-1}	Group 2 50 mg·kg^{-1}
Potassium 4.5–6.0 (mmol·L^{-1})	3.4 ± 0.1	3.3 ± 0.2	3.1 ± 0.3
Glucose 0.89–1.83 (g·L^{-1})	1.07 ± 0.24	0.99 ± 0.14	1.05 ± 0.19
Urea 0.32–0.54 (g·L^{-1})	0.54 ± 0.16	0.44 ± 0.12	0.43 ± 0.02*
Creatinine 3.9–22.9 (mg·L^{-1})	3.3 ± 0.9	3.0 ± 0.3	2.7 ± 0.6
Total proteins 59.0–84.0 (g·L^{-1})	53.8 ± 3.1	54.3 ± 3.3	54.3 ± 2.7
Albumin 32.0–43.0 (g·L^{-1})	38.5 ± 1.9	38.5 ± 2.0	38.8 ± 2.1
PA 39–216 (UI·L^{-1})	80.8 ± 17.8	79.5 ± 20.4	72.5 ± 19.5
TGO 39–92 (UI·L^{-1})	73.8 ± 19.0	69.2 ± 17.5	63.7 ± 5.4
TGP 17–50 (UI·L^{-1})	25.8 ± 7.3	20.8 ± 7.1	25.0 ± 6.9
Total cholesterol 0.5–1.0 (g·L^{-1})	0.7 ± 0.2	0.7 ± 0.2	0.7 ± 0.2
Bile salts 0–40 (μM)	9.82 ± 5.12	8.5 ± 3.66	6.88 ± 2.75
Amylase (UI·L^{-1})	963.3 ± 52.3	884.8 ± 55.3	938.0 ± 110.3

* $p<0.05$ compared to the control group (non-parametric Mann–Whitney test; GraphPad Prism 5.0 software).

long term pattern, a linear increase of excreted Si shows that by the end of the subacute experiment there is 45% more excreted SiC than at the beginning. Given the lack of increase in food consumption or damage to the GI tract, these results point out to a reduced retention of SiC in the GI tract with time.

PIXE measurements offer the advantage of multi-elemental acquisition, and thus all the elements found in the feces were acquired from Mg up to zinc (Zn). A response to the administration of SiC was observed in the rats as a change in the concentration of some elements in the excreted feces with respect to the control group. This response to SiC administration is divided in a short term and a long term response. The short term response was observed in the increase of excreted K (up to 60%) from the acute administration. No significant changes in K were found in the subacute administration, but it was observed that the fecal Ca, P, and Mg excretion was time dependent and increased (up to 29, 18, and 39% at day 28 for Ca, P, and Mg, respectively), probably due to a decreased absorption of these elements as a result of SiC administration. These increments present an increasing statistical significance, especially at day 28 (end of the subacute study) with respect to the other days. A decrease in the absorption of Ca and P is of special importance because both Ca^{++} and PO_4^{-3} ions control the many essential cellular processes (Clapham, 2007). Such decreases in Ca and P, although not inducing an immediate short term toxicity effect or perceptible damage on either the GI tract or liver and kidneys, may have some long term repercussions such as changes in the mitochondrial function, apoptotic cell death or bone metabolism (Clapham, 2007). Magnesium is involved in the synthesis of DNA, RNA and proteins, and plays a complementary role with Ca as a long-term regulatory element (Saris et al., 2000). The increase of excreted Mg (39% increase at day 28 with respect to day one), along with the increase of Ca and P are signs of possible long-term effects in bone metabolism and cellular signaling, which could lead to pathological conditions. Reddy and coworkers found that Ca, P and Mg are reduced in feces excretion for rats without intestinal microflora (Reddy et al., 1969), implying that the rats in this study were not affected in their intestinal microflora.

The biodistribution of SiC was studied in liver, kidneys and spleen using PIXE for a single dose of SiC. These organs are important for the translocation of NPs from the intestinal barrier to the bloodstream and their eventual renal filtration; for example the liver is the primary organ involved in the metabolism and detoxification of xenobiotics (Sahu, 2009). While no trace of Si was detected in any organ, small variations in the levels of P, S, Cl, K and Ca were found in all organs. These variations, excepting Ca, seem to fluctuate given the values for days one and seven. At day one the liver has an excess of these elements (compared to their control values) while both kidneys and spleen show a reduction (except Cl in the kidneys). These trends are reversed at seven days (except Cl in the kidneys, which increased further). In the case of the liver, the levels of P, S, Cl, and Ca from control samples present statistically significant variations between days 1 and 7. Only the level of Cl at day 1 presents a statistically significant variation between the exposed and control samples. In the case of the kidneys, the dosed samples between days 1 and 7 statistically present significant variations in the level of P, S, and Cl. In the case of the spleen, P, S, Cl, and K are significantly different between the dosed and control samples, and between the dosed samples from days 1 and 7. It is apparent that the amount of Ca is lower for both the liver and kidneys even after seven days of SiC administration. It is not clear if this is the case for the spleen. Additionally the amount of Ca in all organs tends to control values with time, as evidenced by the increase in Ca between days 1 and 7. It is apparent that the elemental variations resulting from an acute exposure to SiC in the liver, spleen and kidney lead to fluctuations around the control values, showing that a response from the rats to a single administration of SiC can be traced in organs even seven days after administration and elimination of the dose. The origin of this response should be further investigated. Some possible mechanisms could be size- and Si/C ratio-dependent redox perturbation and DNA damage, as showed by an *in vitro* study on pulmonary cells (A549) exposed to SiC dispersions in ultrapure sterile water (Barillet et al., 2010a).

In the present study SiC was found able to cross from the intestinal barrier and reach the blood stream, given the low traces found in urine. Other NMs have been found to cross the intestinal barrier, like Au NPs (Hillyer and Albrecht, 2001). Studies with carbon-based NMs have similarly found a low percentage cross of the intestinal barrier, like carbon nanotubes (Carrero-Sánchez et al., 2006; Wang et al., 2004) and ^{14}C functionalized fullerenes which were 98% cleared in feces within 48 h and the other 2% excreted through urine (Oberdörster et al., 2005a; Yamago et al., 1995).

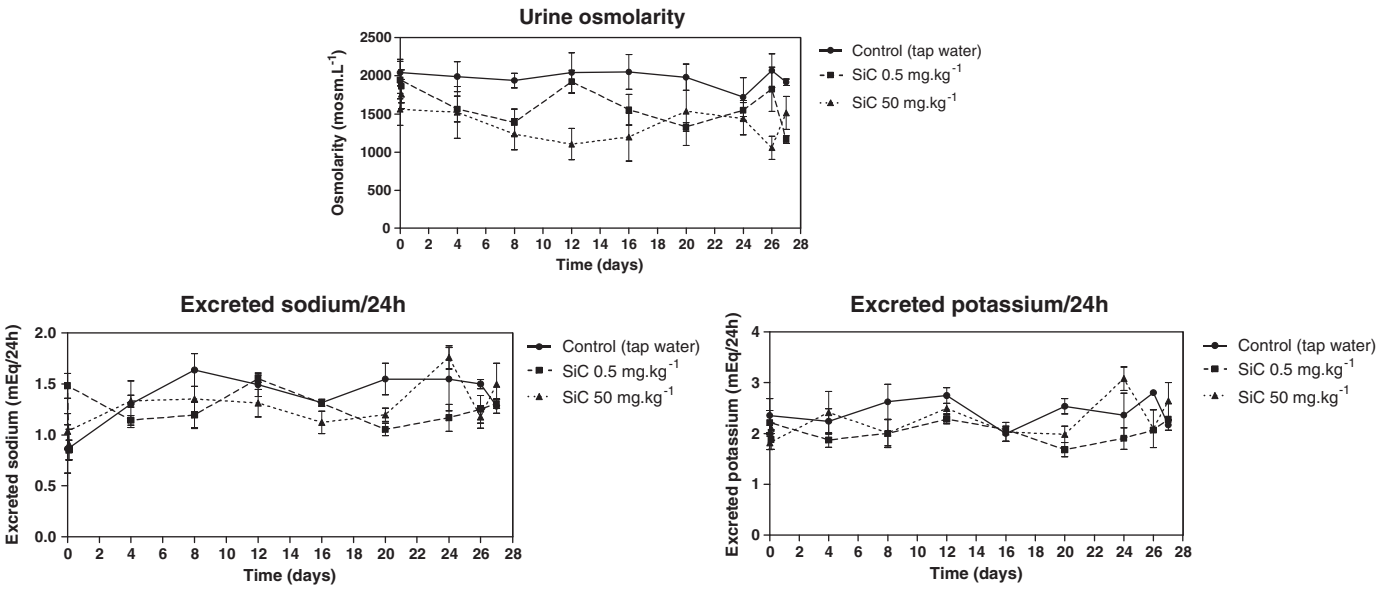

Fig. 11. Daily osmolarity, sodium and potassium excretion over 28 days. Mean ± SD, n = 3. (●) shows the data from the control group; (■) shows the data from the 0.5 mg·kg^{-1} SiC treated group and (▲) shows the data from the 50 mg·kg^{-1} SiC treated group.

Toxicity

Acute and subacute *in vivo* oral administration assessments are of high relevance in light of the potential toxicological effects that NMs can exert, such as: the capacity of NMs to pass cross the intestinal barrier (Hillyer and Albrecht, 2001), the possible accumulation and damage such NMs can exert in key organs (GI tract, liver, kidneys, spleen) and the cardiovascular system (Oberdörster et al., 2005a, 2005b), their effects in blood serum (Kim et al., 2008), and the possible alteration to urinary parameters (potassium, sodium, osmolarity) as an alternative to track down the effects of NMs in the bloodstream. The toxicity apparently is dependent on the type of NM. For example, it has been found that some metal NMs are highly toxic in acute assessments, *i.e.* Zn NPs (Wang et al., 2006, 2008); and similarly metal oxide NPs, like some forms of silica (SiO_2), induce toxicity after subacute assessments (Dekkers et al., 2011).

The present study found that the tested SiC did not induce any morphological alterations like an increase of granulomas or tissue damage to the GI tract, liver, kidneys, and spleen. The lack of morphological alterations in the GI tract is explained due to the fast elimination of SiC through feces excretion. The lack of morphological alterations to liver, kidneys, and spleen can be explained in light of the low amount of SiC crossing the intestinal barrier as inferred from the low traces of SiC in urine and the lack of SiC accumulation in the organs as found in this study.

The alteration of blood biochemical parameters reveals modifications in the blood enzymes, which may indicate a series of events, like a systemic leakage from intracellular sites or target tissues due to cellular or tissue injury (Dandekar et al., 2010). In the present study, the acute assessment, showed no change in serum biochemical parameters, while for the subacute assessment a decrease in the blood concentration of urea was observed for the high dose group (50 mg·kg^{-1}) with respect to the control group. Yet no alteration of renal morphology was observed. These effects seem to be dependent on the NM used, as a study found that silver NPs and titanium dioxide NPs can induce anomalies in liver serum biochemical parameters respectively in rats and mice (Kim et al., 2008). The urinary sodium and potassium elimination, as well as the urine osmolarity were not altered. Therefore it can be concluded that the tested SiC, within the scope of this study, did not induce toxic effects to the exposed rats.

Summary

The biodistribution, toxicity, and elemental composition changes in feces and organs due to orally administered SiC were studied in a rat model. SiC is able to pass across the intestinal barrier, as corroborated in the urine inspection by FEG-SEM-EDX, yet still most of the SiC is excreted by feces. The use of PIXE was crucial to quantify the SiC which was not radiolabeled, radioactivated or fluorescent. SiC quantification revealed a reduction in its retention rate with time through the GI tract, and that a single dose can be mostly eliminated on the first day of administration. In addition PIXE was useful to detect the changes in absorption of Ca, P, and Mg, three elements that are crucial in ionic form in the great majority of cellular processes, measured the lack of SiC accumulation in different organs (liver, kidneys and spleen), and to observe the small yet statistically significant changes in the composition of these organs up to seven days later as a response to the oral administration of SiC. This NM did not induce any morphological alteration in the studied organs (esophagus, stomach, intestines, liver, spleen and kidney), nor an increase in the amount of granulomas. Plasma analyses, in the subacute assessment, showed that SiC induced a small reduction in the amount of urea when compared to the control group. The urinary sodium and potassium elimination, as well as the urine osmolarity were not altered. This lack of alterations shows that this SiC product presents no signs of toxicity in both acute and subacute studies in rats for all the studied doses.

Conflict of interest statement

There is no conflict of interest.

Acknowledgments

This work was supported by the Service Public de Wallonie (SPW) – Direction générale opérationnelle – Economie, Emploi et Recherche (DGO6), Département des Programmes de Recherche (Nanotoxico Project, SPW/FUNDP research convention No. 516252). The authors acknowledge financial support from the European Union under the Framework 7 program through the projects QNano INFRASTRUCTURE-2010-1-262163. O. Toussaint is a Research Associate of the Belgian FNR/FNRS.

Appendix A

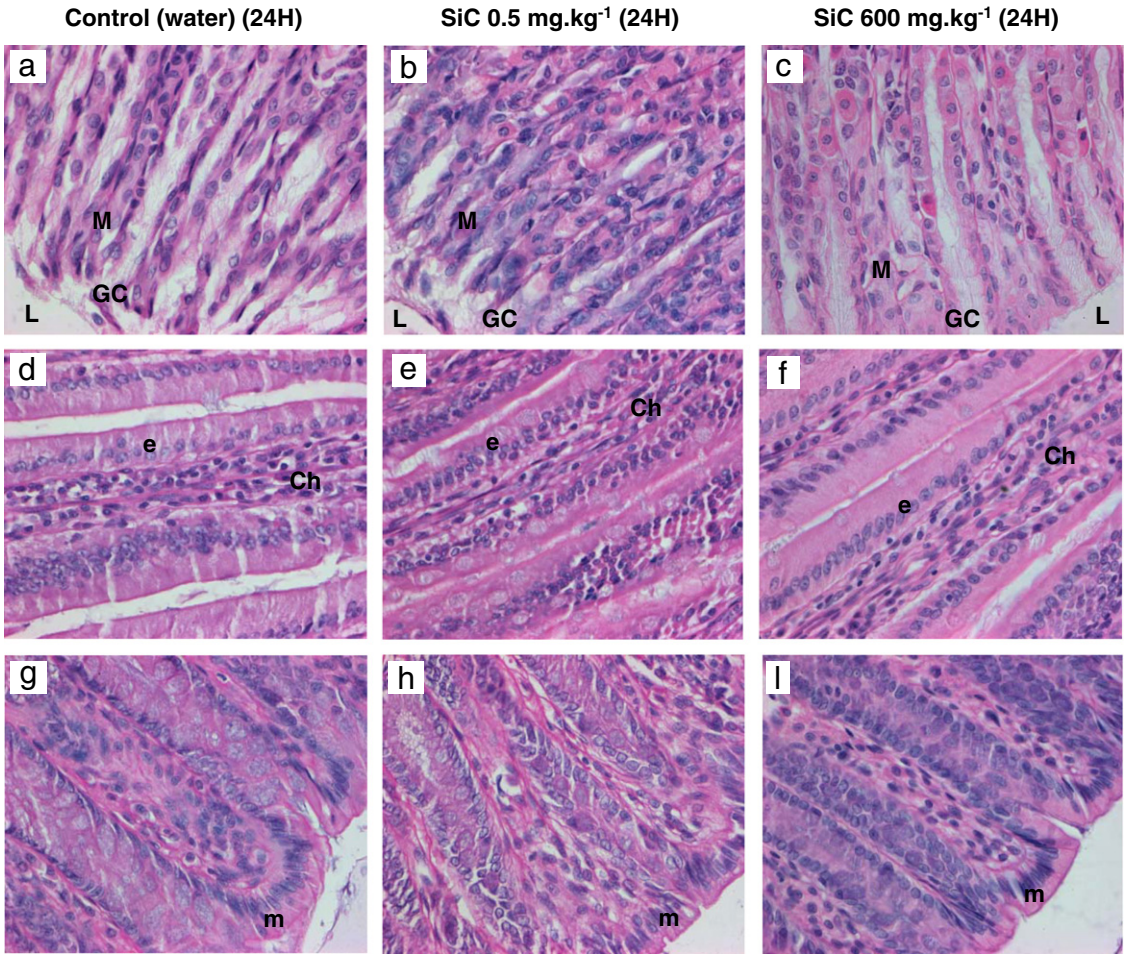

Fig. A.1. Histopathological examination of the stomach (a-c), small intestine (d-f) and large intestine (g-l) of control SiC exposed groups from selected animals: Control group, 0.5 and 600 mg · kg^{-1} exposed groups. L = lumen; Ch = chorion; GC = gastric crypt; M = mucus secreting cells (lining the gastric crypt); e = enterocytes forming the simple cylindrical epithelium; and m = mucosa. H&E, ×400.

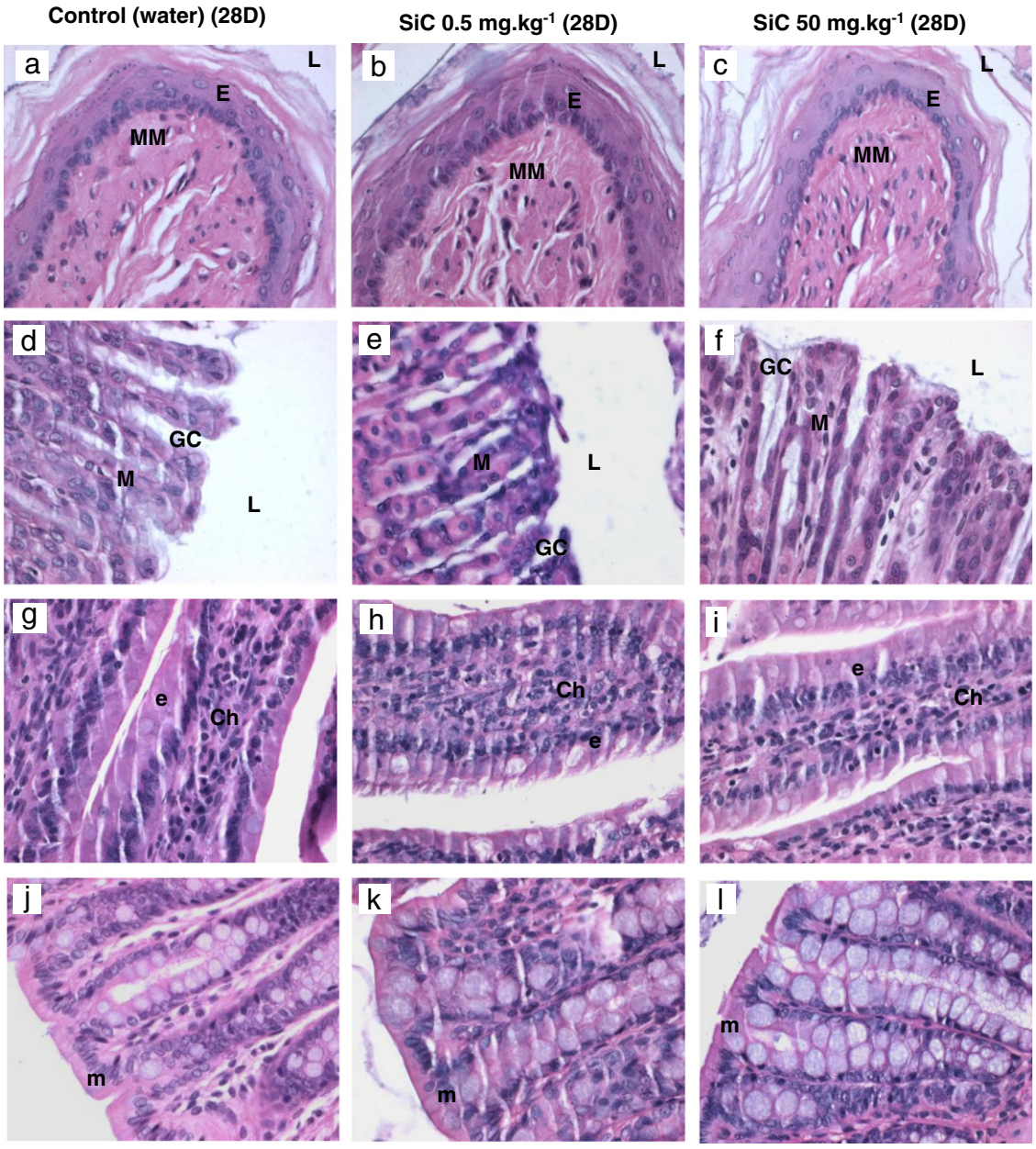

Fig. A.2. Histopathological examination of the esophagus (a-c), stomach (d-f), small intestine (g-i) and large intestine (j-l) of SiC treated animals (0.5 and 50 mg·kg^{-1}) compared to control animals. E = thick keratinized stratified squamous epithelium; L = lumen; MM = muscularis mucosa; GC = gastric crypt; M = mucus secreting cells (lining the gastric crypt); Ch = chorion; e = enterocytes of the simple cylindrical epithelium; and m = mucosal absorptive cells and mucus secreting goblet cells. H&E, ×400.

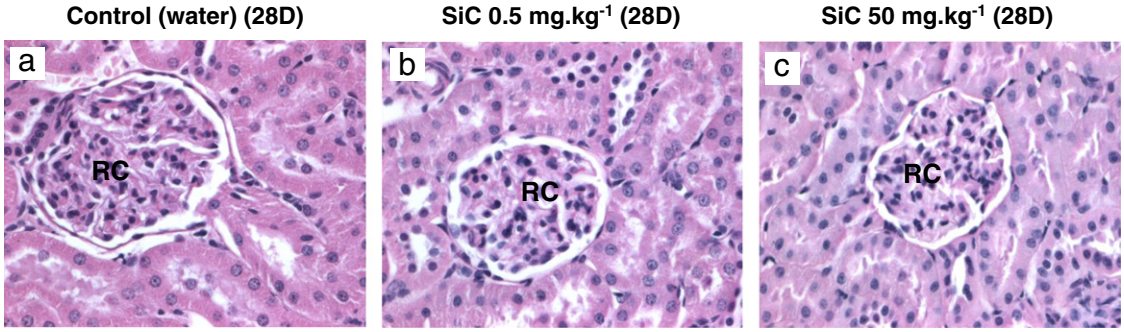

Fig. A.3. Histopathological examination of the kidney (renal cortex) of control, 0.5 and 50 mg·kg^{-1} SiC treated animal. RC = renal corpuscles. H&E, ×400.

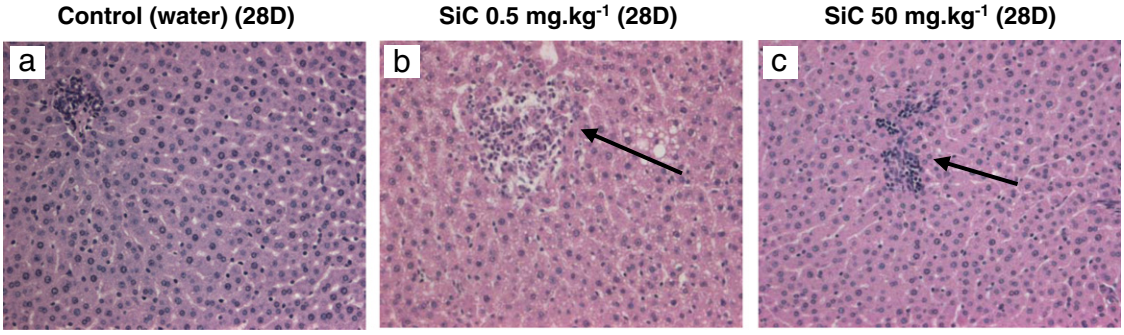

Fig. A.4. Histopathological examination of the liver of control, 0.5 and 50 mg·kg^{-1} SiC treated animal. H&E, ×200.

References

Avila, A.G., Hinestroza, J.P., 2008. Smart textiles: tough cotton. Nat. Nanotechnol. 3, 458–459.

Bagwe, R., Hilliard, L., Tan, W., 2006. Surface modification of silica nanoparticles to reduce aggregation and nonspecific binding. Langmuir 22, 4357–4362.

Barillet, S., Jugan, M.L., Laye, M., Leconte, Y., Herlin-Boime, N., Reynaud, C., Carrière, M., 2010a. *In vitro* evaluation of SiC nanoparticles impact on A549 pulmonary cells: cyto-, genotoxicity and oxidative stress. Toxicol. Lett. 198, 324–330.

Barillet, S., Simon-Deckers, A., Herlin-Boime, N., Mayne-L'Hermite, M., Reynaud, C., Cassio, D., Gouget, B., Carrière, M., 2010b. Toxicological consequences of TiO_2, SiC nanoparticles and multi-walled carbon nanotubes exposure in several mammalian cell types: an *in vitro* study. J. Nanopart. Res. 12, 61–73.

Brown, J., Zeman, K., Bennett, W., 2002. Ultrafine particle deposition and clearance in the healthy and obstructed lung. Am. J. Respir. Crit. Care Med. 166, 1240–1247.

Carrero-Sánchez, J.C., Elías, A.L., Mancilla, R., Arrellín, G., Terrones, H., Laclette, J.P., Terrones, M., 2006. Biocompatibility and toxicological studies of carbon nanotubes doped with nitrogen. Nano Lett. 6, 1609–1616.

Churg, A., Stevens, B., Wright, J.L., 1998. Comparison of the uptake of fine and ultrafine TiO_2 in a tracheal explant system. Am. J. Physiol. 274, L81–L86.

Clapham, D.E., 2007. Calcium signaling. Cell 131, 1047–1058.

Dandekar, P., Dhumal, R., Jain, R., Tiwari, D., Vanage, G., Patravale, V., 2010. Toxicological evaluation of pH-sensitive nanoparticles of curcumin: Acute, sub-acute and genotoxicity studies. Food and Chemical Toxicology 48, 2073–2089.

Dekkers, S., Krystek, P., Peters, R.J.B., Lankveld, D.P.K., Bokkers, B.G.H., van Hoeven-Arentzen, P.H., Bouwmeester, H., Oomen, A.G., 2011. Presence and risks of nanosilica in food products. Nanotoxicology 5, 393–405.

Fan, J., Li, H., Jiang, J., So, L.K., Lam, Y.W., Chu, P.K., 2008. 3C–SiC nanocrystals as fluorescent biological labels. Small 4, 1058–1062.

Galuszka, J., Jarczyk, L., Rokita, E., Strzalkowski, A., Sych, M., 1984. The influence of target preparation and mode of irradiation on PIXE analysis of biological samples. Nucl. Instrum. Methods Phys. Res. B 3, 141–146.

Geraci, C.L., Castranova, V., 2010. Challenges in assessing nanomaterial toxicology: a personal perspective. Wiley Interdiscip. Rev. Nanomed. Nanobiotechnol. 2, 569–577.

Greaves, P., 2007. Liver and Pancreas. In: Histopathology of preclinical toxicity studies. Elsevier Inc., CA, 457–503.

Heublein, B., Pethig, K., Elsayed, A.M., 1998. Silicon carbide coating – a semiconducting hybrid design of coronary stents – a feasibility study. J. Invasive Cardiol. 10, 255–262.

Hillyer, J.F., Albrecht, R.M., 2001. Gastrointestinal persorption and tissue distribution of differently sized colloidal gold nanoparticles. J. Pharm. Sci. 90, 1927–1936.

International Atomic Energy Agency, 1989. Reference materials catalogue and documents. Available from the website: http://curem.iaea.org/catalogue/TE/TE_001530000.html. Accessed on 28th March 2012.

International Atomic Energy Agency, 1990. Reference materials catalogue and documents. Available from the website: http://curem.iaea.org/catalogue/TE/TE_001550000.html. Accessed on 28th March 2012.

Kim, Y.S., Kim, J.S., Cho, H.S., Rha, D.S., Kim, J.M., Park, J.D., Choi, B.S., Lim, R., Chang, H.K., Chung, Y.H., Kwon, I.H., Jeong, J., Han, B.S., Yu, I.J., 2008. Twenty-eight-day oral toxicity, genotoxicity, and gender-related tissue distribution of silver nanoparticles in Sprague–Dawley rats. Inhal. Toxicol. 20, 575–583.

Krinke, G.J., Bullock, G.R., Bunton, T., 2000. The Laboratory Rat (Handbook of Experimental Animals). Academic Press, London.

Lozano, O., Mejia, J., Masereel, B., Toussaint, O., Lison, D., Lucas, S., 2012. Development of a PIXE analysis method for the determination of the biopersistence of SiC and TiC nanoparticles in rat lungs. Nanotoxicology 6, 263–271 (doi:210.3109/17435390.17432011.17572301).

Lynch, I., Dawson, K.A., 2011. Protein–nanoparticle interactions. Nano Today 3, 40–47.

Mejia, J., Tichelaar, F., Saout, C., Toussaint, O., Masereel, B., Mekhalif, Z., Lucas, S., Delhalle, J., 2011. Effects of the dispersion methods in Pluronic F108 on the size and the surface composition of MWCNTs and their implications in toxicology assessment. J. Nanopart. Res. 13, 655–667.

Mejia, J., Valembois, V., Piret, J.P., Tichelaar, F., van Huis, M., Masereel, B., Toussaint, O., Delhalle, J., Mekhalif, Z., Lucas, S., 2012. Are stirring and sonication pre-dispersion methods equivalent for *in vitro* toxicology evaluation of SiC and TiC? J. Nanopart. Res. 14, 815–832.

Mezey, E., 1982. Liver disease and protein needs. Annu. Rev. Nutr. 2, 21–50.

Monopoli, M.P., Walczyk, D., Campbell, A., Elia, G., Lynch, I., Bombelli, F.B., Dawson, K.A., 2011. Physical–chemical aspects of protein corona: relevance to *in vitro* and *in vivo* biological impacts of nanoparticles. J. Am. Chem. Soc. 133, 2525–2534.

Nel, A., Xia, T., Mädler, L., Li, N., 2006. Toxic potential of materials at the nanolevel. Science 311, 622–627.

Nel, A.E., Madler, L., Velegol, D., Xia, T., Hoek, E.M., Somasundaran, P., Klaessig, F., Castranova, V., Thompson, M., 2009. Understanding biophysicochemical interactions at the nano-bio interface. Nat. Mater. 8, 543–557.

Oberdörster, G., 2001. Pulmonary effects of inhaled ultrafine particles. Int. Arch. Occup. Environ. Health 74, 1–8.

Oberdörster, G., Maynard, A., Donaldson, K., Castranova, V., Fitzpatrick, J., Ausman, K., Carter, J., Karn, B., Kreyling, W., Lai, D., Olin, S., Monteiro-Riviere, N., Warheit, D., Yang, H., 2005a. Principles for characterizing the potential human health effects from exposure to nanomaterials: elements of a screening strategy. Part. Fibre Toxicol. 2, 8.

Oberdörster, G., Oberdörster, E., Oberdörster, J., 2005b. Nanotoxicology: an emerging discipline evolving from studies of ultrafine particles. Environ. Health Perspect. 113, 823–839.

Oberdörster, G., Stone, V., Donaldson, K., 2007. Toxicology of nanoparticles: a historical perspective. Nanotoxicology 1, 2–25.

Organisation for Economic Co-operation and Development (OECD), 1995. OECD guideline for testing of chemicals. Repeated dose 28-day oral toxicity study in rodents. Guideline 407 Available from the website: http://www.oecd.org/dataoecd/50/41/37477972.pdf. Accessed on 28th March 2012.

Organisation for Economic Co-operation and Development (OECD), 2001. OECD guideline for testing of chemicals. Acute oral toxicity fixed dose procedure. Guideline 420 Available from the website: http://iccvam.niehs.nih.gov/SuppDocs/FedDocs/OECD/OECD_GL420.pdf. Accessed on 28th March 2012.

Reddy, B.S., Pleasants, J.R., Wostmann, B.S., 1969. Effect of intestinal microflora on calcium, phosphorus and magnesium metabolism in rats. J. Nutr. 99, 353–362.

Sahu, S., 2009. Hepatotoxic potential of nanomaterials. Nanotoxicity: From *In Vivo* and *In Vitro* Models to Health Risks. John Wiley & Sons, Chichester.

Saris, N.E., Mervaala, E., Karppanen, H., Khawaja, J.A., Lewenstam, A., 2000. Magnesium: an update on physiological, clinical and analytical aspects. Clin. Chim. Acta 294, 1–26.

Sharp, P.E., La Regina, M.C., 1998. The Laboratory Rat. CRC Press. 1–204.

Shiga, A., Ota, Y., Ueda, Y., Hosoi, M., Miyajima, R., Hasegawa, K., Mizuhashi, F., 2010. Study on the pathogenesis of foreign body granulomatous inflammation in the livers of sprague-dawley rats. J. Toxicol. Pathol. 23, 253–260.

Shimoda, K., Park, J.-S., Hinoki, T., Kohyama, A., 2007. Influence of surface structure of SiC nano-sized powder analyzed by X-ray photoelectron spectroscopy on basic powder characteristics. Appl. Surf. Sci. 253, 9450–9456.

Takenaka, S., Dornhofer-Takenaka, H., Muhle, H., 1986. Alveolar distribution of fly ash and of titanium dioxide after long-term inhalation by Wistar rats. J. Aerosol. Sci. 17, 361–364.

Taurozzi, J.S., Hackley, V.A., Wiesner, M.R., 2011. Ultrasonic dispersion of nanoparticles for environmental, health and safety assessment — issues and recommendations. Nanotoxicology http://dx.doi.org/10.3109/17435390.2010.528846.

Taylor, T.N., 1989. The surface composition of silicon carbide powders and whiskers: an XPS study. J. Mater. Res. 4, 189–203.

Wang, H., Wang, J., Deng, X., Sun, H., Shi, Z., Gu, Z., Liu, Y., Zhao, Y., 2004. Biodistribution of carbon single-wall carbon nanotubes in mice. J. Nanosci. Nanotechnol. 4, 1019–1024.

Wang, B., Feng, W.Y., Wang, T.C., Jia, G., Wang, M., Shi, J.W., Zhang, F., Zhao, Y.L., Chai, Z.F., 2006. Acute toxicity of nano- and micro-scale zinc powder in healthy adult mice. Toxicol. Lett. 161, 115–123.

Wang, B., Feng, W., Wang, M., Wang, T., Gu, Y., Zhu, M., Ouyang, H., Shi, J., Zhang, F., Zhao, Y., Chai, Z., Wang, H., Wang, J., 2008. Acute toxicological impact of nano- and submicro-scaled zinc oxide powder on healthy adult mice. J. Nanopart. Res. 10, 263–276.

Wang, W., Zhang, S., Chinwangso, P., Advincula, R.C., Lee, T.R., 2009. Electric potential stability and ionic permeability of SAMs on gold derived from bidentate and tridentate chelating alkanethiols. J. Phys. Chem. C 113, 3717–3725.

Yamago, S., Tokuyama, H., Nakamura, E., Kikuchi, K., Kananishi, S., Sueki, K., Nakahara, H., Enomoto, S., Ambe, F., 1995. *In vivo* biological behavior of a water-miscible fullerene: ^{14}C labeling, absorption, distribution, excretion and acute toxicity. Chem. Biol. 2, 385–389.